*J. Fluid Mech.* (1981), *vol.* 103, *pp.* 225–239
*Printed in Great Britain*


# Magnetohydrodynamic secondary flows at high Hartmann numbers

By P. TABELING AND J. P. CHABRERIE

Laboratoire de Génie Électrique de Paris, des Universités Paris VI et Paris XI, Laboratoire associé au C.N.R.S., E.S.E. Plateau du Moulon, 91 190 Gif-sur Yvette, France

(Received 5 March 1979 and in revised form 17 March 1980)

Laminar flows in annular ducts of rectangular cross-section subjected to a constant axial magnetic field $\mathbf{B}_0$ are considered. The equations of flow are treated by a perturbation method involving infinite series expansions in ascending powers of the ratio $\lambda = a/R_0$ (where $a$ and $R_0$ are respectively the height and the mean radius of the annular duct).

The leading terms of the series are calculated in the range of high values of the Hartmann number $M$ by means of a boundary-layer technique. When $M$ is large, the secondary flow pattern exhibits two profoundly distinct features. Firstly, in the Hartmann and interior regions, secondary flows have a one-dimensional structure and involve no inertial effects if the curvature of the duct is small enough; secondly, in thin layers near the walls parallel to the magnetic field, the secondary flow pattern is dramatically influenced by the conductivities of the walls: varying these conductivities gives rise to either one or several counter-rotating eddies. When the Reynolds number of the flow increases, inertial effects emanating from these layers penetrate the core of the duct by convective transport. Order-of-magnitude arguments show that the mean velocity is affected by secondary flow effects when $KM^{-\frac{1}{4}}$ becomes large, where $K$ is the Dean number of the flow.

## 1. Introduction

The problem of laminar secondary flows within curved ducts has attracted much interest over the last few decades. The main reason lies in the fact that theoretical studies give at least qualitative information about real flows commonly encountered in engineering devices: turbomachinary blade passages, diffusers, heat exchangers, etc.

In hydrodynamics, extensive theoretical and experimental work has been carried out on the subject for various shapes of the cross-section of the duct (round, elliptic, rectangular). In contrast only very little has been published in magnetohydrodynamics. The most comprehensive study on the subject has been performed by Baylis & Hunt in 1971. In a first paper, Baylis (1971) carried out experiments on electromagnetically driven flows in curved ducts subjected to an axial, constant magnetic field. He showed that the magnetic field tends to damp secondary flows provided it is strong enough. This was justified in a later paper (Baylis & Hunt 1971) by order-of-magnitude arguments. However, in such an analysis, the authors underestimated secondary flow effects emanating from layers near the walls parallel to the magnetic field. When the

0022-1120/81/4628-3330 $02.00 

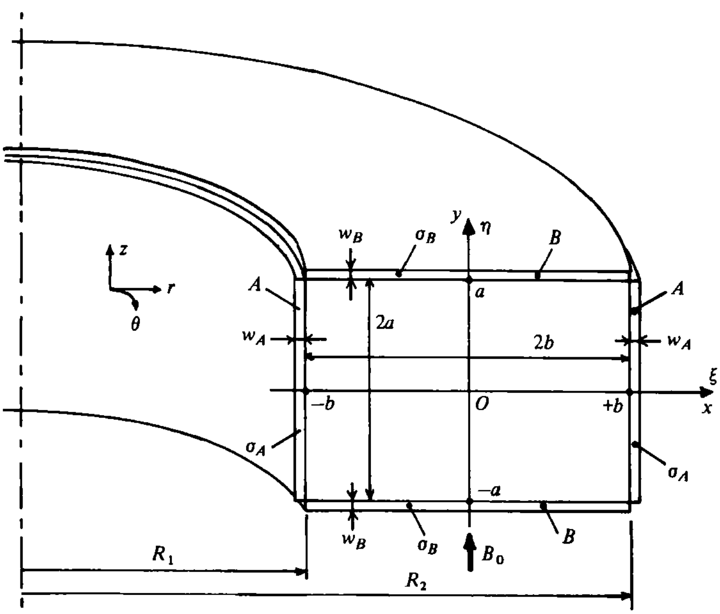


FIGURE 1. Duct geometry and co-ordinate system.

Dean number is sufficiently large, Baylis (1971) showed that friction-factor laws are of hydrodynamic type, i.e. are not affected by the magnetic field. Recently, Tabeling & Chabrerie (1978*a*) extended the experiments of Baylis to the case of rectangular ducts of various aspect ratios, and observed similar results.

The objective of the present paper is to investigate in detail magnetohydrodynamic secondary flows of liquid metals. We shall consider hereafter laminar flows in curved ducts of rectangular cross-section subjected to a strong uniform axial magnetic field.

In § 1 we derive the equations of the problem. In § 2 we introduced the perturbation scheme, and in §§ 3, 4 and 5 we obtain the first two terms of the corresponding expansions. Secondary flow effects are studied in § 6.

## 2. Equations of the problem

We consider steady, fully developed laminar flows of liquid metal in annular ducts of rectangular cross-section (see figure 1). We set $Oz$ as the axis of revolution of the torus, and use polar co-ordinates $r$, $\theta$, $z$. The walls of the duct, located at $r = R_1, R_2$ and $z = \pm a$, are assumed to be symmetrically identical and we denote each pair of them by a single letter $A$ or $B$ (see figure 1); their conductivities and thicknesses are respectively $\sigma_A$, $w_A$ and $\sigma_B$, $w_B$. In addition we assume that $w_A \ll a$ and $w_B \ll a$.

The duct is subjected to a constant uniform magnetic field $B_0$ applied in the $Oz$ direction and the fluid is driven by a constant pressure gradient $\partial P/\partial\theta$ in the azimuthal direction.

We set up the governing equations of the flow subject to the following assumptions: first, the flow is axisymmetric, so that all $\theta$-derivatives are identically zero except that for the pressure $P$. Further, we consider the case of very low magnetic Reynolds number $R_m = \sigma\mu_0 U^* a$, where $\sigma$, $\mu_0$ and $U^*$ are the fluid conductivity, the vacuum permittivity and a characteristic velocity scale. This later assumption allows us to neglect in the equations of flow the induced magnetic field compared to $\mathbf{B}_0$. We replace then the Lorentz forces $\mathbf{J}\times\mathbf{B}$ by $\mathbf{J}\times\mathbf{B}_0$ (where $\mathbf{J}$ is the current density and $\mathbf{B}_0$ the magnetic field), and the induced electrical field $\mathbf{U}\times\mathbf{B}$ by $\mathbf{U}\times\mathbf{B}_0$ (where $\mathbf{U}$ is the velocity field). The resulting equations can be written in terms of $U_r$, $U_\theta$, $U_z$, $P$ and $H_\theta$ (where $H_\theta$ is the $\theta$-component of the magnetic field). We find:

$$U_r\frac{\partial U_r}{\partial r}+U_z\frac{\partial U_r}{\partial z}-\frac{U_\theta^2}{r} = -\frac{\sigma B_0^2}{\rho}U_r-\frac{1}{\rho}\frac{\partial P}{\partial r}+\nu\left(\Delta U_r-\frac{U_r}{r^2}\right), \tag{1}$$

$$U_r\frac{\partial U_\theta}{\partial r}+U_z\frac{\partial U_\theta}{\partial z}+\frac{U_\theta U_r}{r} = \frac{B_0}{\rho}\frac{\partial H_\theta}{\partial r}-\frac{1}{\rho}\frac{\partial P}{r\,\partial\theta}+\nu\left(\Delta U_\theta-\frac{U_\theta}{r^2}\right), \tag{2}$$

$$U_r\frac{\partial U_z}{\partial r}+U_z\frac{\partial U_z}{\partial z} = -\frac{1}{\rho}\frac{\partial P}{\partial z}+\nu\Delta U_z, \tag{3}$$

$$\Delta H_\theta-\frac{H_\theta}{r^2}+\sigma B_0\frac{\partial U_\theta}{\partial z} = 0, \tag{4}$$

and

$$\frac{\partial U_r}{\partial r}+\frac{U_r}{r}+\frac{\partial U_z}{\partial z} = 0. \tag{5}$$

Here $\Delta$ denotes the Laplacian operator expressed in polar co-ordinates, i.e.

$$\Delta = \frac{\partial^2}{\partial r^2}+\frac{1}{r}\frac{\partial}{\partial r}+\frac{\partial^2}{\partial z^2}.$$

$\rho$ and $\nu$ are respectively the volumetric mass density and the kinematic viscosity.

Using the thin-wall approximation (Shercliff 1956), the boundary conditions are: on $r = R_1, R_2$:

$$U_r = U_0 = U_z = 0, \quad \frac{\partial U_\theta}{\partial r}+\frac{H_\theta}{r} = \pm\frac{\sigma}{\sigma_A w_A}H_\theta; \tag{6}$$

and on $z = \pm a$:

$$U_r = U_\theta = U_z = 0, \quad \frac{\partial H_0}{\partial z} = \mp\frac{\sigma}{\sigma_B w_B}H_\theta. \tag{7}$$

It is convenient at this stage to introduce the stream function $\phi$ defined by

$$U_r = -\frac{\partial\phi}{\partial z} \quad\text{and}\quad U_z = \frac{1}{r}\frac{\partial}{\partial r}(r\phi). \tag{8}$$

Now we introduce the following dimensionless quantities:

$$\left.\begin{aligned} u_r^* &= \frac{\tilde{\eta}^3 R_0^2}{\rho a^5(-\partial P/\partial\theta)^2}U_r; \quad u_\theta^* = \frac{\tilde{\eta}R_0}{a^2(-\partial P/\partial\theta)}U_\theta; \quad u_z^* = \frac{\tilde{\eta}^3 R_0^2}{\rho a^5(-\partial P/\partial\theta)^2}U_z;\\ h_\theta^* &= \frac{\tilde{\eta}^{\frac{1}{2}}R_0}{a^2\sigma^{\frac{1}{2}}(-\partial P/\partial\theta)}H_\theta; \quad p^* = \frac{\tilde{\eta}^2 R_0^2}{\rho a^4(-\partial P/\partial\theta)^2}P; \quad \varphi^* = \frac{\tilde{\eta}^3 R_0^2}{\rho a^6(-\partial P/\partial\theta)^2}\phi; \end{aligned}\right\} \tag{9}$$

$$\xi = (r-R_0)/a; \quad \eta = z/a; \quad c = b/a; \quad \lambda = a/R_0; \tag{10}$$

$M = B_0 a(\sigma/\tilde{\eta})^{\frac{1}{2}}$ (Hartmann number), and $Q = (-\partial P/\partial\theta)\rho a^3/R_0\tilde{\eta}^2$ where $\tilde{\eta}$ is the viscosity of the fluid. Using these new quantities, the system (1)–(6) becomes:

$$Q^2\left[u_r^*\frac{\partial u_r^*}{\partial\xi}+u_z^*\frac{\partial u_r^*}{\partial\eta}\right]-\frac{\lambda u_\theta^{*2}}{1+\lambda\xi} = -M^2u_r^*-\frac{\partial\phi^*}{\partial\xi}+\Delta^*u_r^*-\frac{\lambda^2u_r^*}{(1+\lambda\xi)^2}, \tag{11}$$

$$Q^2\left[u_r^*\frac{\partial u_\theta^*}{\partial\xi}+u_r\frac{\partial u_\theta^*}{\partial\eta}+\lambda\frac{u_r^*u_\theta^*}{1+\lambda\xi}\right] = \frac{1}{1+\lambda\xi}+M\frac{\partial h_\theta^*}{\partial\eta}+\Delta^*u_\theta^*-\frac{\lambda^2u_\theta^*}{(1+\lambda\xi)^2}, \tag{12}$$

$$Q^2\left[u_r^*\frac{\partial u_z^*}{\partial\xi}+u_z\frac{\partial u_z^*}{\partial\eta}\right] = -\frac{\partial p^*}{\partial\eta}+\Delta^*u_z^*, \tag{13}$$

$$\Delta^*h_\theta^*-\frac{\lambda^2h_\theta^*}{(1+\lambda\xi)^2}+M\frac{\partial u_\theta^*}{\partial\eta} = 0, \tag{14}$$

$$\frac{\partial u_r^*}{\partial\xi}+\lambda\frac{u_r^*}{1+\lambda\xi}+\frac{\partial u_z^*}{\partial\eta} = 0, \tag{15}$$

together with (see (6), (7)):

$$u_r^* = u_\theta^* = u_z^* = 0,\quad \frac{\partial h_\theta^*}{\partial\xi}+\lambda\frac{h_\theta^*}{1+\lambda\xi} = \mp D_A h_\theta^*,\quad \xi = \pm c; \tag{16}$$

$$u_r^* = u_\theta^* = u_z^* = 0,\quad \frac{\partial h_\theta^*}{\partial\eta} = \mp D_B h_\theta^*,\quad \eta = \pm 1; \tag{17}$$

where

$$\Delta^* = \frac{\partial^2}{\partial\xi^2}+\frac{\lambda}{1+\lambda\xi}\frac{\partial}{\partial\xi}+\frac{\partial^2}{\partial\eta^2},$$

$$D_A = \frac{\sigma a}{\sigma_A w_A} \quad\text{and}\quad D_B = \frac{\sigma a}{\sigma_B w_B}.$$

## 3. The expansion scheme in series in ascending powers of $\lambda$

The following formal method of resolution can be applied to the equations (11)–(15): Consider a function $g^*$ related to the problem, and expand it as an infinite series in ascending powers of $\lambda$:

$$g^* = g^{(0)}+\lambda g^{(1)}+\lambda^2 g^{(2)}+\ldots+\lambda^n g^{(n)}+\ldots. \tag{18}$$

The convergence of this series will be discussed in §6. (18) defines a perturbation scheme in term of $\lambda = a/R_0$; the leading term $g^{(0)}$ is calculated by setting $\lambda = 0$ directly in the problem and hence corresponds to a flow developing in a rectilinear geometry; we shall describe this as the 'primary flow'. The subsequent terms, $g^{(1)}, \ldots, g^{(n)}$, describe the curvature effects.

## 4. The leading term (primary flow) in the asymptotic case $M \gg 1$ and $M^{\frac{1}{2}}c \gg 1$

Setting $\lambda = 0$ in the problem, we find:

$$\left.\begin{aligned} u_r^{(0)} = u_z^{(0)} = \partial p^{(0)}/\partial\xi = \partial p^{(0)}/\partial\eta = 0,\\ \partial^2u_\theta/\partial\xi^2+\partial^2u_\theta/\partial\eta^2+M\,\partial h_\theta/\partial\eta = -1,\\ \partial^2h_\theta/\partial\xi^2+\partial^2h_\theta/\partial\eta^2+M\,\partial u_\theta/\partial\eta = 0, \end{aligned}\right\} \tag{19}$$

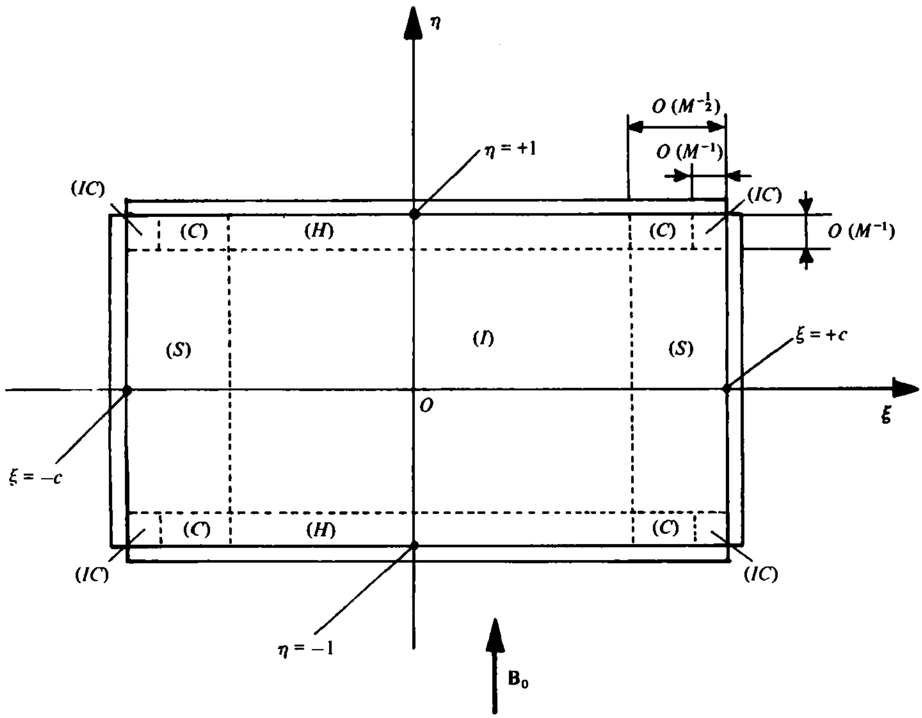


FIGURE 2. Cross-section of the duct showing the various regions of the flow when $M \gg 1$ and $M^{\frac{1}{2}}c \gg 1$.

together with

$$
\left.\begin{aligned}
& u_\theta = 0, \quad \partial h_\theta/\partial\xi = \mp D_A h_\theta, \quad \xi = \pm c; \\
\text{and} \qquad & u_\theta = 0, \quad \partial h_\theta/\partial\eta = \mp D_B h_\theta, \quad \eta = \pm 1.
\end{aligned}\right\} \tag{20}
$$

In this system as well as in the following equations we omit the exponent (0) for $u_\theta$ and $h_\theta$.

The system (19), (20) has been extensively analyzed for various values of $D_A$ and $D_B$. We shall restrict ourselves to the asymptotic case in which $M \gg 1$ and $M^{\frac{1}{2}}c \gg 1$, i.e. where magnetohydrodynamic effects are the most significant. In this case, the flow exhibits the following distinct regions (Temperley & Todd 1971) (see figure 2):

($I$) Interior region, including most of the fluid, but excluding the boundary layers on the walls of the duct.

($H$) Hartmann layers, of thickness $O(M^{-1})$, near the walls $BB$, excluding regions distant $O(M^{-\frac{1}{2}})$ from the pair of side walls $AA$.

($S$) Secondary layers of thickness $O(M^{-\frac{1}{2}})$, near the walls $AA$.

($C$) Corner regions, i.e. those parts of the Hartmann layers at a distance $O(M^{-\frac{1}{2}})$ from the side walls $AA$.

($IC$) Inner corner regions, i.e. those parts of the duct at a distance $O(M^{-1})$ from the corners.

It turns out that $u_\theta(\xi, \eta)$ can be decomposed (Temperley & Todd 1971) as

$$
u_\theta(\xi,\eta) = u_{\theta I}(\xi,\eta) + u_{\theta H}(\xi,\eta') + u_{\theta S}(\xi',\eta) + u_{\theta C}(\xi',\eta') + u_{\theta IC}(t,\eta'). \tag{21}
$$

in which $u_{\theta I}$ is the interior velocity and $u_{\theta H}$, $u_{\theta S}$, $u_{\theta C}$, $u_{\theta IC}$ are perturbations describing the flow in the region denoted by the subscripts; $\xi'$, $\eta'$ and $t$ are inner co-ordinates defined by $\xi' = M^{\frac{1}{2}}(c-\xi)$, $\eta' = M(1-\eta)$ and $t = M(c-\xi)$ for the quarter-plane $\xi \geqslant 0$, $\eta \geqslant 0$, similar expressions holding for the other parts of the duct. By definition, all perturbations as well as their derivatives are negligible outside their regions of influence.

The flow is uniform in the interior region and it decreases exponentially in Hartmann layers. We have (Temperley & Todd 1971):

$$u_{\theta I}(\xi,\eta) = u_I = \frac{1+D_B}{M(D_B+M)} \quad \text{and} \quad u_{\theta H}(\xi,\eta') = -u_I e^{-\eta'}.$$

In the secondary layers, the problem is more complicated. To first order (in the quarter-plane $\xi \geqslant 0$, $\eta \geqslant 0$), the governing equations for $\mu_{\theta S}$, $h_{\theta S}$ are (Temperley & Todd 1976, Tabeling & Chabrerie 1980*b*):

$$\frac{\partial^2 u_{\theta S}}{\partial \xi'^2}+\frac{\partial h_{\theta S}}{\partial \eta} = 0, \quad \text{and} \quad \frac{\partial^2 h_{\theta S}}{\partial \xi'^2}+\frac{\partial u_{\theta S}}{\partial \eta} = 0, \tag{22}$$

together with:

$$\left.\begin{aligned} &u_{\theta S} = -u_I \quad \text{and} \quad \frac{\partial h_{\theta S}}{\partial \xi'} - D_A M^{-\frac{1}{2}} h_{\theta S} = -D_A M^{-\frac{3}{2}}\eta \quad \xi' = 0;\\ &u_{\theta S}+D_B(D_B+M)^{-1} h_{\theta S} = 0, \quad \eta = 1. \end{aligned}\right\} \tag{23}$$

In corner regions, $u_{\theta C}$ is simply related to $u_{\theta S}$ by

$$u_{\theta C}(\xi',\eta') = -u_{\theta S}(\xi',1)\, e^{-\eta'},$$

which is valid to the first order. The problem can be solved in the $(S)$ and $(C)$ regions without making reference to the $(IC)$ regions (Temperley & Todd 1971). In such regions, $u_{\theta IC}$ is at most of the same order as $u_{\theta S}$.

(22), (23) have been solved by Shercliff (1953) (case $D_A = D_B = \infty$), Hunt (1965) (cases $D_A = \infty$ or $D_B = 0$), Hunt & Stewartson (1965) and Chiang & Lundgren (1967) (case $D_A = 0$ and $D_B = \infty$). Recently, Tabeling & Chabrerie (1980*b*) solved the same system in the general case ($D_A$ and $D_B$ arbitrary), by means of a Galerkin-type approach.

## 5. The first-order term in the expansion scheme (18)

### 5.1. *The governing equations*

The governing equations for the first-order term of (18) are obtained by equating in (11)–(17) all terms of order $\lambda$. The resulting equations are more easily expressed in terms of the velocity function $\varphi^{(1)}$. We obtain:

$$\frac{\partial^4\varphi}{\partial\xi^4}+2\frac{\partial^4\varphi}{\partial^2\xi^2\partial^2\eta^2}+\frac{\partial^4\varphi}{\partial\eta^4}-M^2\frac{\partial^2\varphi}{\partial\eta^2} = \frac{\partial u_\theta^2}{\partial\eta}, \tag{24}$$

with:

$$\varphi = \frac{\partial\varphi}{\partial\xi} = \frac{\partial\varphi}{\partial\eta} = 0 \quad \text{on} \quad \xi = \pm c \quad \text{and} \quad \eta = \pm 1, \tag{25}$$

in which, for simplicity, we have omitted the exponent (1) on $\varphi$. The boundary conditions (25) derive simply from (8), (16), (17) and from the choice of the constant $\varphi = 0$ on the boundaries. From (24), (25) it follows that $\varphi$ is even in $\xi$ and odd in $\eta$.

### 5.2. *Resolution of* (24) *when* $M$, $M^{\frac{1}{2}}c$ *are large*

When $M$ and $M^{\frac{1}{2}}c$ are large, it is natural to suppose the existence of boundary-layer solutions for $\varphi$ of the same type as those for $u_\theta$: this follows from (24). In any event, a definitive check will be obtained by the consistency of the results. Hence, assuming that the flow is divided into five regions (Hartmann, interior, secondary, corner and inner corner regions (see figure 2)), we apply a perturbation method to solve the problem. $\varphi$ is decomposed into five terms as follows:

$$\varphi(\xi,\eta) = \varphi_I(\xi,\eta)+\varphi_H(\xi,\eta')+\varphi_S(\xi',\eta)+\varphi_C(\xi',\eta')+\varphi_{IC}(t,\eta'), \tag{26}$$

in which each subscript denotes the corresponding region of flow; in (26), $\xi'$, $\eta'$ and $t$ have the same meaning as in (21). Similar expansions hold for $u_r^{(1)}$, $u_z^{(1)}$ and $p^{(1)}$. Now we examine each region of flow, restricting ourselves to the quarter-plane $\xi > 0$; $\eta > 0$. The expressions for $\xi'$, $\eta'$ and $t$ are then respectively

$$\xi' = M^{\frac{1}{2}}(c-\xi); \quad \eta' = M(1-\eta) \quad \text{and} \quad t = M(c-\xi).$$

5.2.1. *Interior region.* Eliminating in (24) terms of $O(M^{-2})$ compared to $M^2\,\partial^2\varphi/\partial\eta^2$ and making use of the uniformity of the primary flow $u_\theta$ in the interior region, we find

$$-M^2\frac{\partial^2\varphi_I}{\partial\eta^2} = 0. \tag{27}$$

The general form of $\varphi$ is then

$$\varphi_I = \eta f(\xi), \tag{28}$$

where $f(\xi)$ is some even function of $\xi$.

5.2.2. *Hartmann layers.* The governing equation for $\varphi_H$, valid through terms of $O(M^{-2})$, is (see (24), (26)):

$$\frac{\partial^4\varphi_H}{\partial\eta'^4}-\frac{\partial^2\varphi_H}{\partial\eta'^2} = -M^{-3}\frac{\partial}{\partial\eta'}(u_{\theta I}+u_{\theta H})^2, \tag{29}$$

together with:

$$\eta' = 0: \quad \varphi_H(\xi,0) = -\varphi_I(\xi,1) = -f(\xi) \quad \text{(say)}, \quad \frac{\partial\varphi_H}{\partial\eta'} = M^{-1}\frac{\partial\varphi_I}{\partial\eta} = M^{-1}f(\xi)\,\text{(say)}, \tag{30}$$

and $\eta' \to \infty$: $\varphi_H = \partial\varphi_H/\partial\eta' = 0$. In (30), the conditions on the side-wall $\xi = c$ have been omitted as being irrelevant to the problem (see the absence of derivatives in $\xi$ in (29)). Now, using the expression for $u_{\theta I}+u_{\theta H}$ given in § 4, and solving (29) leads to a general solution of the form

$$\varphi_H(\xi,\eta') = A(\xi)\,e^{-\eta'}+\tfrac{1}{6}u_I^2M^{-3}[6(1+\eta')\,e^{-\eta'}+e^{-2\eta'}]. \tag{31}$$

$A(\xi)$, and simultaneously $f(\xi)$, are now determined by using the boundary conditions. We find:

$$A(\xi)+\tfrac{7}{6}u_I^2M^{-3} = -f(\xi) \quad \text{and} \quad A(\xi)+\tfrac{1}{3}u_I^2M^{-3} = -M^{-1}f(\xi). \tag{32}$$

Solving (32) yields

$$f(\xi) = -\tfrac{5}{6}u_I^2M^{-3}(1-M^{-1})^{-1} \tag{33}$$

and

$$A(\xi) = \tfrac{5}{6}u_I^2M^{-3}(1-M^{-1})^{-1}-\tfrac{7}{6}u_I^2M^{-3}. \tag{34}$$

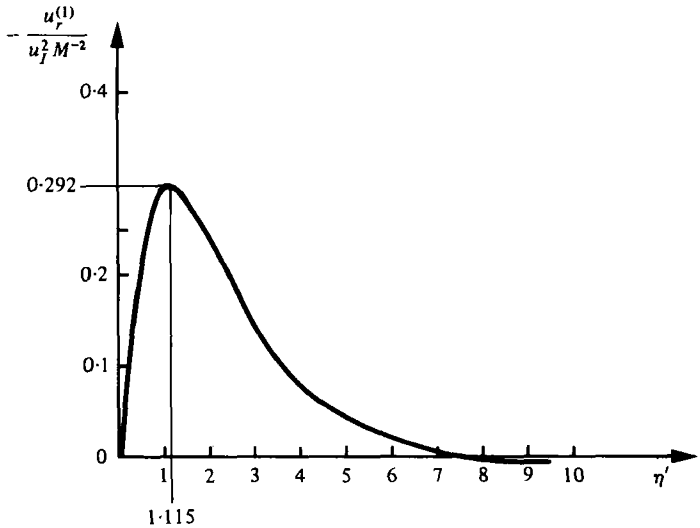


FIGURE 3. Radial velocity profile in the Hartmann layers calculated at $M \cong 500$.

The corresponding expressions for the velocity field are

$$\left.\begin{aligned} u_{rH}^{(1)} &= -\tfrac{1}{6}u_I^2 M^{-2}[6(\eta'-\tfrac{1}{3})\,e^{-\eta'}+2e^{-\eta'}]-\tfrac{5}{6}u_I^2 M^{-3}\,e^{-\eta'}+O(u_I^2 M^{-5}),\\ u_{rI}^{(1)} &= \tfrac{5}{6}u_I^2 M^{-3}+O(u_I^2 M^{-5}) \quad \text{and} \quad u_{zI}^{(1)} = u_{zH}^{(1)} = 0. \end{aligned}\right\} \tag{35}$$

Since the expressions (33) and (34) are independent of $\xi$, these in fact yield the correct solution of equation (24) through exponentially small terms in $M$.

The one-dimensional character of the secondary flows in the ($H$–$I$) regions is due to a mechanism of vorticity suppression by the magnetic field: (27) expresses the fact that the orthoradial component of vorticity is zero in the interior region; this in turn implies suppression of $u_z$ and uniformity of $u_r$. The amplitude of the secondary flows is determined in Hartmann layers, without reference to the other regions of flow. In this sense, such regions are active.

In figure 3, we have plotted the function

$$-\frac{u_r^{(1)}}{u_I^2 M^{-2}} = -\frac{u_{rI}^{(1)}+u_{rH}^{(1)}}{u_I^2 M^{-2}}$$

against $\eta'$, for an arbitrary value of $\xi$ (satisfying $|\xi \pm c| \gg M^{-\frac{1}{2}}$), and a value of $M$ about 500. The curve exhibits an absolute maximum calculated as $\eta' \approx 1{\cdot}1146$ and $M^2 u_r^{(1)}/u_I^2 \approx -0{\cdot}292$. These values are independent of $M$ to first order. In contrast, the point where the flow reverses moves significantly to the right of the plane when $M$ increases. A reasonable estimate of the position of such a point is $\eta' \sim \log M$. Up to this point, as $M$ increases the profiles flatten, their general form remaining otherwise unchanged.

5.2.3. *The secondary region.* The complete governing equation for $\varphi_s$ is (see (24), (25), (26))

$$M^{-2}\frac{\partial^4\varphi_s}{\partial\eta^4}+2M^{-1}\frac{\partial^4\varphi_S}{\partial\xi'^2\,\partial\eta^2}+\frac{\partial^4\varphi_s}{\partial\xi'^4}-\frac{\partial^2\varphi_s}{\partial\eta^2} = M^{-2}\frac{\partial}{\partial\eta}(u_{\theta I}+u_{\theta S})^2, \tag{36}$$

together with
$$\varphi_S = \tfrac{5}{8}u_I^2 M^{-3}\eta \quad \text{and} \quad \partial\varphi_S/\partial\xi' = 0, \quad \xi' = 0. \tag{37}$$

Anticipating the study of the corner region, we impose the following condition (which will be justified later) on $\eta = 1$:

$$\varphi_S(\xi', 1) = -\tfrac{5}{8}M^{-3}u_{\theta S}(\xi', 1)\,[2u_I + u_{\theta S}(\xi', 1)] + O(u_{\theta S}^2 M^{-4}). \tag{38}$$

Now, considering only the most significant part of $\varphi_S$, we neglect in (36) the first two terms of the left-hand side and find the approximate form of (36) to the first order:

$$\frac{\partial^4 \varphi_S}{\partial \xi'^4} - \frac{\partial^2 \varphi_S}{\partial \eta^2} = M^{-2}\frac{\partial}{\partial \eta}(u_{\theta I} + u_{\theta S})^2. \tag{39}$$

Since $u_{\theta I}$ is at most of the same order of $u_{\theta S}$, we can estimate the contribution of the right-hand side term of (39) to the solution $\varphi$ as $O(u_{\theta S}^2 M^{-2})$. It follows that we can replace (37) and (38) by

$$\varphi_S = \partial\varphi_S/\partial\xi' = 0 \quad \text{on} \quad \xi' = 0 \quad \text{and} \quad \varphi_S = 0 \quad \text{on} \quad \eta = 1, \tag{40}$$

which are correct to the first order. The solution of (39), (40) is found to be

$$\varphi_S = \sum_{p=1}^{\infty}\left[\phi_p(\xi') - \frac{1}{\beta_p}\,\phi_p'(0)\,e^{-\beta_p\xi'}\sin\beta_p\xi'\right]\sin\alpha_p\eta, \tag{41}$$

in which $\alpha_p = p\pi$, $\beta_p = (p\pi/2)^{\frac{1}{2}}$, and $\phi_p(\xi')$ is defined by

$$\phi_p(\xi') = \frac{4}{\pi}\int_0^\infty \frac{A_p(\omega)}{\omega^4 + \alpha_p^2}\sin(\omega\xi')\,d\omega, \tag{42}$$

where

$$A_p(\omega) = -\alpha_p M^{-2}\int_0^1\int_0^\infty [u_I + u_{\theta S}(s,t)]^2\cos\alpha_p t\sin\omega s\,ds\,dt. \tag{43}$$

In (41), $\phi_p'(0)$ denotes the usual derivative of $\phi_p'(\xi')$ at $\xi' = 0$.

A first result which emerges from the present analysis is that secondary flows are far more intense in secondary regions than in Hartmann and interior regions (see the ratio $\varphi_S/\varphi_I$ which is at least $O(M)$). Such a feature can be understood by examining the equation (24): in the interior region, $\partial u_\theta^2/\partial\eta$ is zero; it takes significant values only in thin Hartmann layers where viscous effects are strong. On the other hand, in secondary regions such a term takes significant values on much larger scales than in Hartmann regions. The viscous action is in turn weaker and the secondary flows more intense.

The expressions (41), (42), (43) have been computed in various cases: (*a*) all walls insulating ($D_A = D_B = \infty$), (*b*) walls $AA$ insulating, walls $BB$ conducting ($D_A = \infty$; $D_B = 0$) and (*c*) all walls perfectly conducting ($D_A = D_B = 0$). The relevant expressions for $u_{\theta S}$ are those stated by Shercliff (1953) and Hunt (1965). In cases (*a*) and (*c*) primary flow profiles are universal, whereas in case (*b*) they change with $M$. In this latter case we have taken $M = 200$ for the purpose of computation. These three cases should be sufficiently representative.

In figure 4, we show the streamlines $\hat{\varphi}_S = cst$ on the plane $\xi' > 0$, $\eta > 0$, where $\hat{\varphi}_s$ is defined by

$$\hat{\varphi}_S = M^2 u_I^{-2}\varphi_S \text{ in cases } (a), (c) \quad \text{and} \quad \hat{\varphi}_S = u_I^{-2}\varphi_S \text{ in case } (b).$$

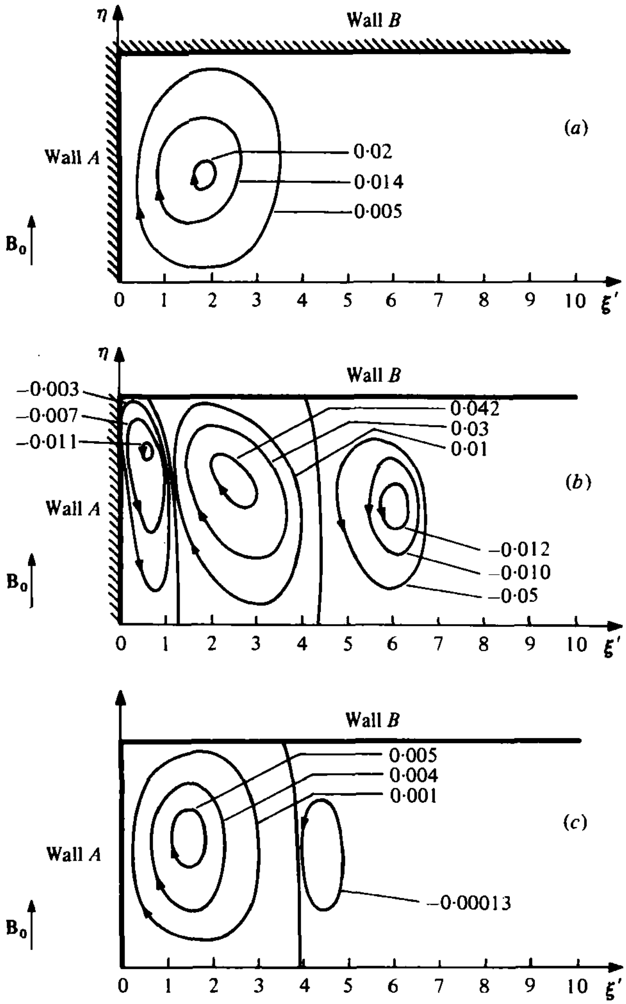


FIGURE 4. Secondary flow pattern in the secondary layer $\xi > 0$ for various values of the conductivities of the walls: (*a*) all walls insulating; (*b*) walls *BB* conducting, walls *AA* insulating; (*c*) all walls conducting. \\\\\\\\\\, insulating walls.

It turns out that secondary streamlines are dramatically influenced by the conductivities of the walls. In case (*a*) there is a single eddy (figure 4*a*), whereas in cases (*b*) and (*c*) there are several counter-rotating eddies with exponentially decreasing amplitude as $\xi' \rightarrow \infty$ (figures 4*b*, *c*).

The secondary streamlines are closely related to the form of the forcing term $\partial u_\theta^2/\partial\eta$. This latter is represented in figure 5 as a function of $\xi'$ at $\eta = 0{\cdot}5$. (On the ordinate, the circumflex notation has the same meaning as that for $\varphi_S$). In case (*a*), $\partial u_{\theta S}^2/\partial\eta$ is everywhere positive giving rise to the single vortex of figure 4*a*, whereas in the other cases the forcing term has the form of a damped sine wave with changes of sign giving rise to counter-rotating vortices. A similar analysis can be done for the amplitudes. If $\mathscr{A}(f)$ is the maximum amplitude of $f$, our computations indicate that

$$\mathscr{A}(\hat{\varphi}) = (0{\cdot}1\text{–}0{\cdot}2) \times \mathscr{A}(\partial u_{\theta S}^2/\partial\eta).$$

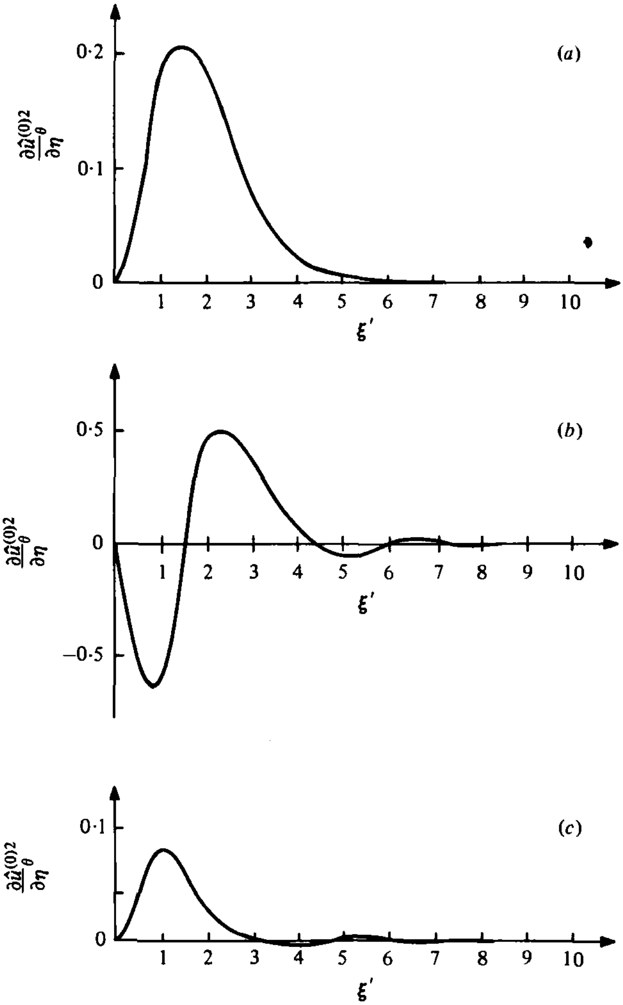


FIGURE 5. The curl of the centrifugal forces in the secondary layer for various values of the conductivities of the walls: (*a*) all walls insulating; (*b*) walls *BB* conducting, walls *AA* insulating; (*c*) all walls conducting.

Since $\mathscr{A}(\partial u^2_{\theta S}/\partial\eta)$ lies in the range 0·05–0·5 in all cases, the levels of amplitude of the secondary flows are in turn rather small; we find

(*a*) $D_A = D_B = \infty$: $\hat{\phi}_{S\max} \approx 0{\cdot}021$; $\hat{u}_{r\max} \approx 0{\cdot}11$,

(*b*) $D_A = \infty$, $D_B = 0$: $\hat{\phi}_{S\max} \approx 0{\cdot}041$; $\hat{u}_{r\max} \approx 0{\cdot}18$,

(*c*) $D_A = D_B = 0$: $\hat{\phi}_{S\max} \approx 0{\cdot}006$; $\hat{u}_{r\max} \approx 0{\cdot}021$.

We have not considered the case when walls *BB* are insulating and walls *AA* conducting, since primary flow profiles are then close to those of case (*a*) (Chiang & Lundgren 1967), the secondary flow pattern should not differ dramatically from that of figure 4(*a*).

The close relationship between $\partial u^2_{\theta S}/\partial\eta$ and secondary flows in the *S* region shows that these latter are effectively 'driven' by the curl of the centrifugal forces. Essentially, such a feature is due to the absence of inertial terms in (24). We shall return to this point later.

5.2.4. *The corner and inner corner regions.* As no novelty is involved, we write directly the governing equation for $\varphi_c$ to the first order:

$$\frac{\partial^4\varphi_c}{\partial\eta'^4}-\frac{\partial^3\varphi_c}{\partial\eta'^2} = -2M^{-3}u_{\theta S}(\xi',1)\,[2u_I+u_{\theta S}(\xi',1)]\,(e^{-\eta'}-e^{-2\eta'}), \tag{44}$$

with

$$\partial\varphi_C/\partial\eta' = 0 \quad \text{and} \quad \varphi_C = -\varphi_S(\xi',1), \quad \eta' = 0. \tag{45}$$

The general solution of (44) is

$$\phi_c(\xi',\eta') = C(\xi')\,e^{-\eta'}+\tfrac{1}{6}M^{-3}u_{\theta S}(\xi',1)\,[2u_I+u_{\theta S}(\xi',1)]\,[6(1+\eta')\,e^{-\eta'}+e^{-2\eta'}],$$

where $C(\xi')$ is an arbitrary function of $\xi'$. Using (45) determines both $C(\xi')$ and $\varphi_S(\xi',1)$. To first order we find

$$\varphi_s(\xi',1) = -\tfrac{5}{6}M^{-3}u_{\theta S}(\xi',1)\,[2u_I+u_{\theta S}(\xi',1)].$$

This yields the required condition on $\eta = 1$, and hence justifies (38).

In the inner corner region, it can be shown that $\varphi_{IC}$ is at most $O(u_{\theta S}^2 M^{-3})$.

## 6. Secondary flow effects in the narrow-gap case

We study now higher-order terms of the expansion scheme (18) under the narrow-gap assumption, i.e. in the range of small values of $\lambda' = \lambda c$. In such a case we have

$$1+\lambda\xi = 1+O(\lambda') \sim 1; \quad \frac{\partial}{\partial\xi}+\frac{\lambda}{1+\lambda\xi} = \frac{\partial}{\partial\xi}+O(\lambda') \sim \frac{\partial}{\partial\xi},$$

similar statements holding for the higher derivatives. The system (11)–(15) can be approximated (in terms of $u_\theta^*$, $h_\theta^*$ and $\varphi^*$) by

$$Q^2\left[-\frac{\partial\varphi^*}{\partial\eta}\frac{\partial}{\partial\xi}(\Delta\varphi^*)+\frac{\partial\varphi^*}{\partial\xi}\frac{\partial}{\partial\eta}(\Delta\varphi^*)\right]+\lambda\frac{\partial u_\theta^{*2}}{\partial\eta} = -M^2\frac{\partial^2\varphi^*}{\partial\eta^2}+\Delta^2\varphi^*, \tag{46}$$

$$Q^2\left[-\frac{\partial\varphi^*}{\partial\eta}\frac{\partial u_\theta^*}{\partial\xi}+\frac{\partial\varphi^*}{\partial\xi}\frac{\partial u_\theta^*}{\partial\eta}\right] = 1+M\frac{\partial h_\theta^*}{\partial\eta}+\Delta u_\theta^*, \tag{47}$$

and

$$\Delta h_\theta^*+M\frac{\partial u_\theta^*}{\partial\eta} = 0, \tag{48}$$

where

$$\Delta = \partial^2/\partial\xi^2+\partial^2/\partial\eta^2,$$

together with homogeneous boundary conditions derived from (16), (17).

Next, applying the perturbation scheme (18) to the above system yields the following recurrence relations (valid for $n \geqslant 1$):

$$\Delta^2\phi^{(n)}-M^2\frac{\partial^2\phi^{(n)}}{\partial\eta^2} = 2\sum_{p=1}^{n-1}u_\theta^{(p)}\frac{\partial u_\theta^{(n-p)}}{\partial\eta}+Q^2\sum_{p=1}^{n-1}\left[\frac{\partial\varphi^{(p)}}{\partial\eta}\frac{\partial}{\partial\xi}(\Delta\varphi^{(n-p)}+\frac{\partial\varphi^{(p)}}{\partial\xi}\frac{\partial}{\partial\eta}(\Delta\phi^{(n-p)})\right], \tag{49}$$

$$\left.\begin{aligned}\Delta u_\theta^{(n)}+M\frac{\partial h_\theta^{(n)}}{\partial\eta} &= Q^2\sum_{p=1}^{n}\left[-\frac{\partial\varphi^{(p)}}{\partial\eta}\frac{\partial u_\theta^{(n-p)}}{\partial\xi}+\frac{\partial\varphi^{(p)}}{\partial\xi}\frac{\partial u_\theta^{(n-p)}}{\partial\eta}\right],\\ \Delta h_\theta^{(n)}+M\,\partial u_\theta^{(n)}/\partial\eta &= 0,\end{aligned}\right\} \tag{50}$$

with homogeneous boundary conditions on $\xi = \pm c$ and $\eta = \pm 1$. (49), (50) can be solved by an iterative method: knowing $u_\theta^{(0)}, h_\theta^{(0)}, \phi^{(1)}$, gives $u_\theta^{(1)}, h_\theta^{(1)}$ (see (50)) and, next, using (49) leads to $\phi^{(2)}$, etc. Such a calculation involves formidable algebra; however, we can obtain the orders of magnitude of $u_\theta^{(n)}$ and $\phi^{(n)}$ in each region of flow by means of such a procedure, provided that (18) converges.

### 6.1. *The interior and Hartmann regions*

Since $\partial u_\theta^{(0)}/\partial\xi$ and $\partial\varphi^{(0)}/\partial\xi$ are zero in $H$–$I$ regions (see § 5), it is easy to show that $u_\theta^{(n)} = h_\theta^{(n)} = \varphi^{(n+1)} = 0$ for any $n \geqslant 1$. It follows that $u_\theta^{(0)}, h_\theta^{(0)}$ and $\phi^{(1)}$ are the exact solution of the problem to any order in $\lambda$ in the range of high-curvature ratios. Such a remarkable feature is essentially due to a mechanism of vorticity suppression by the magnetic field: inertial terms are irrotational in ($HI$) regions, and are simply balanced by a pressure gradient. In other words, there is no *efficient coupling between primary and secondary flows.*

### 6.2. *The secondary layers*

Let us consider the ($S$) region $\xi > 0$ and introduce the inner co-ordinate $\xi' = M^{\frac{1}{2}}(c-\xi)$. The governing system for $\phi^{(n)}, u_\theta^{(n)}, h_\theta^{(n)}$ to the first order is

$$\frac{\partial^4\varphi^{(n)}}{\partial\xi'^4} - \frac{\partial^2\varphi^{(n)}}{\partial\eta^2} = 2M^{-2}\sum_{p=0}^{n-1} u_\theta^{(p)}\frac{\partial u_\theta^{(n-p)}}{\partial\eta} - Q^2M^{-\frac{1}{2}}\sum_{p=1}^{n}\left[-\frac{\partial\varphi^{(p)}}{\partial\eta}\frac{\partial^3\varphi^{(n-p)}}{\partial\xi'^3} + \frac{\partial\varphi^{(p)}}{\partial\xi'}\frac{\partial^3\varphi^{(n-p)}}{\partial\xi'^2\partial\eta}\right], \quad (51)$$

and

$$\left.\begin{aligned} &\frac{\partial^2 u_\theta^{(n)}}{\partial\xi'^2} + \frac{\partial h_\theta^{(n)}}{\partial\eta} = -Q^2M^{-\frac{1}{2}}\sum_{p=1}^{n}\left[-\frac{\partial\varphi^{(p)}}{\partial\eta}\frac{\partial u_\theta^{(n-p)}}{\partial\xi'} + \frac{\partial\varphi^{(p)}}{\partial\xi'}\frac{\partial u_\theta^{(n-p)}}{\partial\eta}\right], \\ &\frac{\partial^2 h_\theta^{(n)}}{\partial\xi'^2} + \frac{\partial u_\theta^{(n)}}{\partial\eta} = 0, \end{aligned}\right\} \quad (52)$$

together with homogeneous boundary conditions. Let us consider two cases: (i) $D_A M^{-\frac{1}{2}}$ not large, $D_B M^{-1}$ not small and (ii) $D_A M^{-\frac{1}{2}}$ large, $D_B M^{-1}$ small.

In case (i), we have $u_\theta^{(0)} \sim u_I$ and $\phi^{(1)} \sim u_I^2 M^{-2}$ (see § 5). Using (52) gives

$$u_\theta^{(1)} \sim u_I Re^2 M^{-\frac{1}{2}},$$

where $Re = u_I a/\nu$ is the Reynolds number of the flow. Repeating this procedure for $\varphi^{(2)}, u_\theta^{(2)}, \ldots, \varphi^{(n)}, u_\theta^{(n)}$, gives

$$u_\theta^{(n)} \sim u_I(Re\, M^{-\frac{1}{4}})^{2n}$$

and

$$\phi^{(n)} \sim u_I M^{-2}(Re\, M^{-\frac{1}{4}})^{2n-2}.$$

The expressions for $u_\theta^*$ and $\varphi^*$ are therefore of the form

$$u_\theta^*/u_I = \sum_{n=0}^{\infty} (KM^{-\frac{1}{4}})^{2n} f^{(n)}(\xi', \eta), \quad (53)$$

and

$$\varphi^*/u_I^2 M^{-2} = \sum_{n=1}^{\infty} (KM^{-\frac{1}{4}})^{2n-2} g^{(n)}(\xi', \eta), \quad (54)$$

where $K = Re\,\lambda^{\frac{1}{2}}$ is the Dean number of the flow, and $f^{(n)}$, $g^{(n)}$ functions of order one. (53), (54) provide the sufficient condition for convergence of the perturbation method:

$$KM^{-\frac{1}{4}} \ll 1. \tag{55}$$

Now, when (55) is satisfied, $u_\theta^{(0)}$ and $\varphi^{(1)}$ represent accurately the solution of the flow within a relative error $O(K^2M^{-\frac{1}{2}})$.

In case (ii), we have $u_\theta^{(0)} \sim Mu_I$ and $\varphi^{(1)} \sim u_I^2$. It suffices then to replace $u_I$ by $Mu_I$ in all the above expressions. (55) remains valid if $K$ is defined as $(Mu_I a/\nu)\,\lambda^{\frac{1}{2}}$ instead of $(u_I a/\nu)\,\lambda^{\frac{1}{2}}$.

(55) can also be viewed as a criterion for inertial effects to be negligible. It is more stringent than the condition stated by Baylis & Hunt (1971) which was $KM^{-\frac{1}{2}} \ll 1$. When $KM^{-\frac{1}{4}}$ becomes large, viscous forces compete with strong inertial forces and this is possible only if the thickness of the boundary layers near the side walls $AA$ decreases; this thickness can be estimated by comparing inertial and viscous stresses, i.e. by formulating a purely hydrodynamical equilibrium. According to previous studies (Ludwieg 1951; Mori, Uchida & Ukon 1971), the thickness is $O(K^{-\frac{1}{2}}) \ll O(M^{-\frac{1}{2}})$. The flow is in turn modified far away from the side-walls $AA$. Further a purely hydrodynamic type flow sets in throughout the duct.

## 7. Summary and conclusion

The present paper gives an analysis of secondary flows in a curved duct subjected to a strong axial magnetic field $\mathbf{B}_0$. It is remarkable that the magnetic field imposes such a simple structure on secondary flows in the main part of the duct ($H$–$I$ regions): in such regions the vorticity has only two components (along $r$ and $z$); inertial terms are ineffectual and secondary flows are simply conveyed by the primary flow without being 'coupled' to it!

In secondary regions, we have profoundly distinct features: such layers are essentially two-dimensional, all components of the vorticity being non-zero; when the Dean number $K$ increases, inertial effects emanating from them penetrate the flow far away from the side-walls; secondary-flow effects become significant when $KM^{-\frac{1}{4}}$ is large enough.

The conclusions of the present paper are in fair agreement with experiments of Baylis (1971) and Tabeling & Chabrerie (1980*a*). (These latter extended the experiments of Baylis to rectangular ducts of various aspect ratios.) It turns out that the 'critical' value of $KM^{-\frac{1}{4}}$ beyond which secondary flow effects become significant is found close to 5 over all the experiments. Note that this relatively high 'critical' value gives also a substantial check for the levels of the secondary flows calculated in § 4 (these latter were found to be rather small).

When $K$ increases until $KM^{-\frac{1}{4}} \gg 1$, Baylis, Tabeling & Chabrerie observed that the flow dissipations are of hydrodynamic type: this is in agreement with the qualitative analysis given above (see § 6).

The stability of secondary flows has not been considered here. Experiments mentioned above show that such flows are stable over a large range of Dean numbers when the walls $AA$ are conducting and the walls $BB$ insulating. The most unstable case should be with walls $AA$ insulating and wall $BB$ conducting, since the primary flow then exhibits inflexion points and reversed profiles (Hunt 1965), and the secondary flow a great number of vortices in thin layers. Some interesting investigations can be carried out on this problem.

We thank Mrs Roussel for the typewriting of the manuscript.

## REFERENCES


BAYLIS, J. A. 1971 *J. Fluid Mech.* **48**, 417.

BAYLIS, J. A. & HUNT, J. C. R. 1971 *J. Fluid Mech.* **48**, 423.

CHIANG, D. & LUNDGREN, T. S. 1967 *Z. angew. Math. Phys.* **18**, 92.

HUNT, J. C. R. 1965 *J. Fluid Mech.* **21**, 563.

LUDWIEG, H. 1951 *Ing. Archiv* **19**, 296.

MORI, Y., UCHIDA, Y. & UKON, T. 1971 *Int. J. Heat Mass Transfer* **14**, 1787.

SHERCLIFF, J. A. 1953 *Proc. Camb. Phil. Soc.* **49**, 136.

SHERCLIFF, J. A. 1956 *J. Fluid Mech.* **1**, 644.

TABELING, P. & CHABRERIE, J. P. 1980*a* *J. Méc.* **19** (**3**), 1.

TABELING, P. & CHABRERIE, J. P. 1980*a* *MHD Flows and Turbulence II* (ed. H. Branover & A. Yakhot), pp. 283–293. Israël University Press.

TEMPERLEY, D. J. & TODD, L. 1971 *Proc. Camb. Phil. Soc.* **69**, 337.

TEMPERLEY, D. J. & TODD, L. 1976 *J. Inst. Math. Applics.* **18**, 309.